J. Chem. Soc. Nigeria, Vol. 46, No.4, pp 0793 – 0802 [2021]

COORDINATION-DRIVEN SELF-ASSEMBLY DISCRETE ORGANOPLATINUM(II) SUPRAMOLECULAR METALLACYCLE

I. J. Mbonu[ab*], Y. Sun[ac], and P. J. Stang[a]

[a]Department of Chemistry, University of Utah, Salt Lake City, UT 84112
[b]Department of Chemistry, Federal University of Petroleum Resources, Efurun, Delta State, Nigeria
[c]School of Chemistry and Chemical Engineering, Yangzhou University, Jiangsu 225002, P.R. China
*Corresponding Author: mbonu.idongesit@fupre.edu.ng

ABSTRACT

The aim of this investigation is, to utilize coordination-driven self-assembly reactions of 4, 4′-dibromobenzophenone with tetrakis(triethyl phosphine) platinum to construct platinum-containing supramolecular metallacycle, 4, 4′-bis[trans-Pt(PEt_3)$_2$Br]benzophenone with exploitable properties for application in catalysis, energy storage, and biomedicine. The process was monitored by ^{1}H NMR and ^{13}C NMR. A 4, 4'-dibromobenzophenone and tetrakis(triethyl phosphine) platinum in the ratio 1:2 in toluene were utilized in the synthesis. In the structure, platinum ions are coordinated through the bridging ligand molecules forming polymeric chains with a four atomic environment. The coordination environment was that of a square planar geometry with two phosphorus atoms of triethyl phosphine in apical positions. The optimized geometry evaluated by DFT B3LYP-6-311G, Gaussian09W, and Avogadro models support the crystal structure of this molecule. The compound offers high reversible binding properties that can be used for designing smart surfaces for applications in catalysis, energy storage, and biomedicine. The results from the experimental investigation and computer-aided design provide insight into the best strategies, by design, and binding mode. Future works are recommended for developing this discrete supramolecular metallacycle into supramolecular metallacages for its application in the drug delivery system.

Keywords: Coordination-driven, self-assembly, supramolecular metallacycle, organoplatinum

INTRODUCTION

Coordination-driven [1-4] self-assembly has evolved into a well-established method for designing novel two-dimensional polygons and three-dimensional polyhedral supramolecular architectures with functional applications in catalysis [5], gas storage [6], drug delivery [7, 8], and molecular electronics. The interest in this method is born out of the accessibility of numerous ligands and metals that are compatible with this technique and of the fact that predetermined structures are formed from this strategy. The efficiency and excellence of this procedure is based on the non-covalent interactions of hydrogen bonding, van der Waals [9] forces, and π-π stacking to form well-defined thermodynamically stable supramolecular structures of various sizes, and shapes. This technique is high-yielding, and the rigid acceptors and donors used in this method aid in maintaining directionality to form single discrete supramolecular architecture [10]. As reported in recent literature [11-13], the metal bonds created by "coordination-driven self-assembly" processes are extremely directional and moderately strong, giving quantitative yields of well-defined pores of varying geometries such as octahedral, polygon, rhomboid, rectangle, square, and triangles. Coordination-driven [6] self-assembly method uses metal acceptors [9] and electron-rich

ISSN 0795 - 22066

donors [11] in union with the non-covalent interactions to create predefined structures. Over the last few decades, the pioneer works of Lehn [14], Stang [2], Huang [7] and others have emerged from the self-assembling processes happening in the biological systems, These scientists have been able to create functional structures such as 2D metalla- macrocycles and metallacages by utilizing "coordination-driven self-assembly" design and method. The design procedures utilized in synthesizing 2D and 3D structures are summarized in Figures 1 and 2. In the construction of 3D architectures, various high-symmetry supramolecular cages such as tetrahedron, octahedron, cube, icosahedrons are obtained (Figures 2 and 3). The non-covalent [14)] interactions between organplatinum compounds and ligands occur through the ligand residues at specific positions located in its pocket-like regions. The particular key ligand residues which are ligand-binding sites [10] have pulled in much consideration in the areas of molecular docking [3], drug-target interactions, compound constructions, ligand affinity prediction [2], and even molecular dynamics. Thus, spotting the ligand [7] binding sites helps to investigate the specificity of intermolecular interactions and also to gain effective insight into the pathogenesis of diseases, which provides understanding for drug discovery [15] and design [10]. The prediction of high-quality structure in conjunction with experimental results is necessary for designing supramolecular architectures with desired applications in biomedicine, energy storage, and catalysis. Researchers have great practical value focusing on optimizing synthesized structures to ultimately improve the success rate on generating supramolecular metallacages and supramolecular metallacyles and for follow-up studies in their targeted properties for applications in industries [16-18]. The aim of this investigation is, to utilize a coordination-driven self-assembly reactions of 4,4′-dibromobenzophenone with tetrakis(triethyl phosphine) platinum to construct platinum-containing supra- molecular metallacycle, 4, 4′-bis[trans-Pt(PEt_3)$_2$Br]benzophenone. Our group recently prepared Pt-supramolecular complex cross-linked by Br-Pt-P and demonstrated the ability to form discrete complex and coordination polymer through coordination-driven [19] self-assembly. We also study the energy levels of this compound with the intentions of using the synthesized supramolecule in energy harvesting and cancer therapeutics.

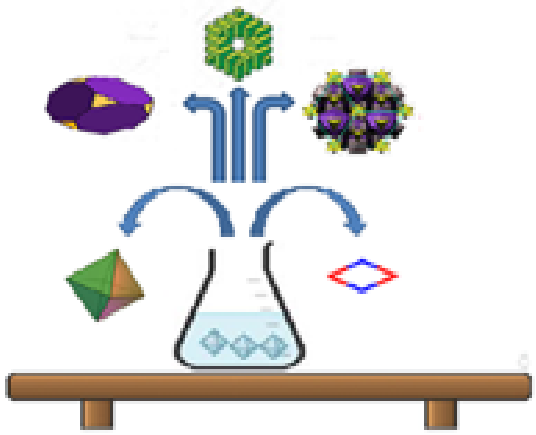

Figure1. Coordination-driven self-assembly of two- and three dimensional- assemblies developed into rectangles, squares, triangles, rhomboids, and polygons geometries

ISSN 0795 - 22066

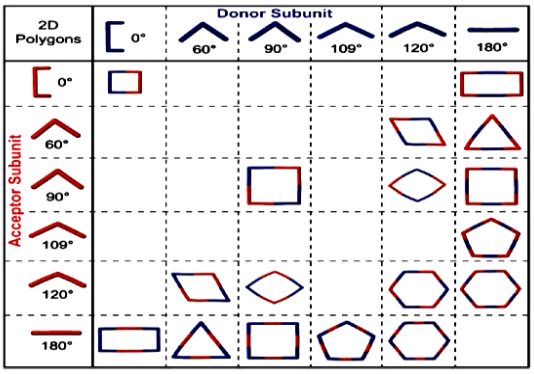

Figure 2. Graphical representations of different building-blocks to Form 2D structures Adapted with permission from references Northrop et al. (2009). Copyright from American Chemical Society

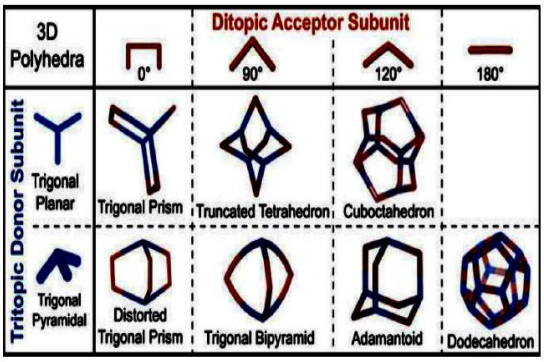

Figure 3. Graphical representations of different building-blocks to Form Structures Adapted with permission from references Northrop et al. (2009). Copyright from American Chemical Society

MATERIALS AND METHODS

All the reagents used in this experiment were purchased commercially and utilized as received. The solvents used in the research work were purified and rendered oxygen-free under nitrogen environment [11]. The organoplatinum supramolecular metallacycle was synthesized according to the published procedure. The NMR spectra [2, 9] were measured on a Varian Unity 300MHZ spectrometer. ^{1}H, and ^{13}C NMR chemical shifts are reported relative to residual solvent signals. The DFT calculations were carried out utilizing Gaussian09W software with B3LYP hybrid and basis set 6-311G [10, 20]. Convergence criteria for geometry optimization, UFF and, single-point calculations were used.

Synthesis of discrete organoplatinum (II) supramolecular metallacycle

The preparation of the organoplatinum (II) supramolecular metallacycle was according to protocols found in the literature [2, 9]. A 1+2.2 mixtures of 4,4'-dibromo-benzophenone and tetrakis(triethyl phosphine) platinum in toluene stirred at room temperature for 6 days led to the formation of self-assembled **[**21] organoplatinum(II) supramolecular metallacycle (see Scheme1). The preparation was performed utilizing the Schlenk technique. The light brown powder is soluble in protonic solvents, including hexane and dichloromethane. The compound was purified using column chromatography. Recrystallization was carried out on the sample after purification [22].

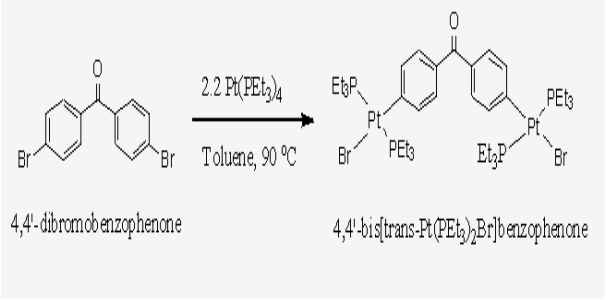

Scheme1. Preparation of discrete organoplatinum (II) supramolecular metallacycle

RESULTS

Figure 4 is an ORTEP view of the organoplatinum (II) supramolecular metallacycle structure with the adopted numbering scheme. Tables 1, 2 and 3 give selected bond angles, atomic data and contact atoms of the synthesized organoplatinum(II) supramolecular metallacyle. The ORTEP view shows the coordination mode of the Pt(II) with a slightly distorted square-planer geometry. This distortion stems from the chelate five-ring constraint imposed by P(25)-Pt-P(33) angle to 102.69°. The Br(16)-Pt-P(25) [104. 56 °] and P(32)-Pt-P(40)

ISSN 0795 - 22066

[104.38yc°] are very close to ideal angles for this geometry. The Pt-Br [2.400 Å and Pt-P[2.3940 Å] are the bond distances [11, 23].

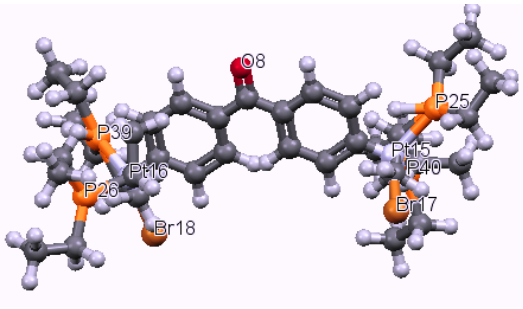

Figure 4: ORTEP plot of organoplatinum (II) compound

Table 1: Selected Bond Angles in Degrees

Bond	Actual(°/A)	optimal(°/A)	Bond	Actual(°/A)	optimal(°/A)
P(46)-H(118)	1.4370	1.4370	C(5)-Pt(16)	1.3460	1.3460
P(33)-H(87)	1.4370	1.4370	C(12)-Pt(15)	1.3460	1.3460
P(26)-H(71)	1.4370	1.4370	C(45)-P(46)	1.8560	1.8560
P(25)-H(70)	1.4370	1.4370	C(43)-P(46)	1.8560	1.8560
C(24)-H(69)	1.1130	1.1130	C(42)-C(43)	1.5230	1.5230
C(24)-H(68)	1.1130	1.1130	C(41)-P(46)	1.8560	1.8560
C(23)-H(67)	1.1130	1.1130	P(33)-C(39)	1.8560	1.8560
C(23)-H(66)	1.1130	1.1130	P(33)-C(37)	1.8560	1.8560
Pt(16)-P(33)	2.3940	2.3940	P(33)-C(35)	1.8560	1.8560
Pt(16)-P(46)	2.3940	2.3940	P(26)-C(32)	1.8560	1.8560
Pt(15)-P(26)	2.3940	2.3940	P(26)-C(30)	1.8560	1.8560
Pt(15)-P(25)	2.3940	2.3940	P(26)-C(28)	1.8560	1.8560
Pt(16)-Br(18)	2.4400	2.4400	C(20)-P(25)	1.8560	1.8560
Pt(15)-Br(17)	2.4400	2.4400			

Table 2. Atomic Data

Pt15	P40	C42	125.68
Pt15	P40	C44	116.31
Pt15	P40	C46	103.44
Pt15	P40	H103	89.47
Br16	Pt14	P25	104.56
Br16	Pt14	P33	102.69
Pt14	P25	C20	107.83
Pt14	P25	C22	111.24
Pt15	P32	C29	103.44
Pt15	P32	C31	85.16
P25	Pt14	P33	109.34
P32	Pt15	P40	104.38
C27	P32	C29	94.26
C29	P32	C31	87.86
C29	P32	H86	105.39
C31	P32	H86	93.36

Table 3: Selected Torsion Barriers (°Å) from optimized structure of organoplatinum(II) compound

Atom type	Bond radii	Angle °	Distance Å	Atom type	Bond radii	Angle °	Distance Å
C-C_R	2.4758	3.031	-0.4498	P-	5.4389	0.0417	-0.817
C-C_R	3.2209	2.0541	0.1293	C-C_3	-6.4478	-1.0294	-2.3995
C-C_R	2.4736	1.0968	0.7436	C-C_3	-6.3269	-1.648	-0.994
C-C_R	-1.4107	-0.1845	0.346	C-C_3	7.9857	5.4462	0.5265
C-C_R	-0.9726	2.1707	0.2185	C-C_3	7.4461	4.0531	0.1848
Pt-Pt4+2	4.5632	2.0385	0.1652	C-C_3	5.1466	3.5961	-3.4281
Pt-Pt4+2	-4.2589	-2.1189	1.4213	C-C_3	6.2137	3.6292	-2.3245
Br-Br	5.1743	1.8838	2.5109	P-	-5.9903	-1.6506	3.006
Br-Br	-2.9194	-3.7174	2.6673	C-C_3	-7.3367	0.873	3.5361
O-O_R	-1.4971	3.249	0.0002	C-C_3	-7.4444	0.4383	2.7427
C-C_3	5.178	-1.2724	-3.3868	C-C_3	-4.6456	-1.197	5.6061
C-C_3	5.0691	0.1035	-2.713	C-C_3	-5.6165	-2.1204	4.8535
C-C_3	6.2484	-2.6513	-0.0775	C-C_3	-7.872	-3.5133	1.6855

Density functional Gaussian 09 orbital approach –Gauss view 5.08 program were used to evaluate the optimal geometry, predict the reaction and nuclear energies of the organoplatinum (II) molecule (Figure 5). The geometry optimization on the prepared supramolecule metallacycle was performed using B3LYP method with the basis set 6-311G (d, p). The results obtained are: nuclear repulsion energy = 1080.9970783412 Hartrees; steric energy = 109.522 Kcal/mol; universal force field of

ISSN 0795 - 22066

organoplatinum (II) compound based on the platinum element, its hybridization, and coordination mode was determined to be = 1.74634635 x 10^{-6} Kcal/mol; degree of freedom= 348; chemical formula: $C_{37}H_{68}Br_2OP_4Pt_2$; rotational constants (GHz): 0.0760179: 0.0133514: 0.0130706; symmetry adapted basis functions of A =397. These results show that the compound has a spin multiplicity of 1 indicating that compound exists in three energy states [10, 24].

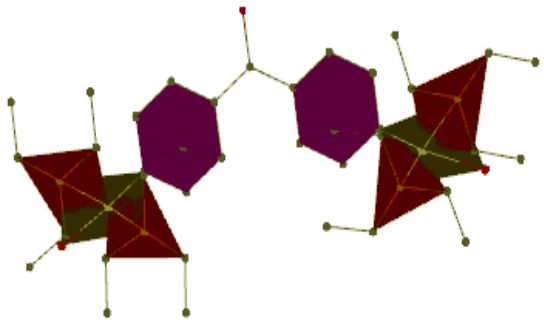

Figure 5: optimized structure of organoplatinum compound

The extent to which a compound goes into a reaction is determined from the energy gap that exists between the highest occupied molecular [25] orbital (HOMO) and lowest unoccupied [26] molecular orbital (LUMO). The E_{HOMO} and E_{LUMO} of the organoplatinum (II) compound is calculated utilizing B3LYP/6-311G [20] (d, p) method.

Figure 6 shows molecular [18] orbitals involved in the chemical reaction: the HOMOs in red is delocalized over carbon atoms to which the PEt_3 groups are attached and the LUMOs in blue are orbitals over carbon atoms to which Br groups are attached. The calculated energy gap (ΔE) [20] of value 2.26 eV represents electronic energy transition belonging to $\pi \rightarrow \pi^*$ excitation. The coordination-driven [4] self-assembly [3, 6] has been utilized to prepare three-dimensional molecular structures with internal cavities or pores capable of trapping ions [27], and other molecules. This encapsulating property and the ability to stabilize other ions and molecules in their cavities makes them potential materials for catalysis, drug delivery, energy storage, and nano-electronic devices. Reactivity can be controlled by encapsulation especially in terms of drug delivery. In order to effectively improve the solubility and stability of platinum (II) under physiological condition while increasing its biocompatibility and bioactivity, methane was encapsulated within the pores of the supramolecular metallacycle. In the aspect of drug delivery, the impact of encapsulating small molecules aids in the regulation of its chemical reaction. The encapsulated molecules are expelled from constrained solvation sphere and placed very close to the host and other guest.

Figure 7 shows encapsulation of methane molecule within the pores [5] of the Pt(II) supramolecular structure. Various drugs [10] including cisplatin can also be encapsulated [22, 28] into the cavities of Pt(II) supramolecule (Figure 7). This exceptionally high surface area with a tunable pore size of Pt(II) supramolecular structure may generate enhanced cooperative catalytic activity, selectivity, and stability for flexible design functionalities [29].

ISSN 0795 - 22066

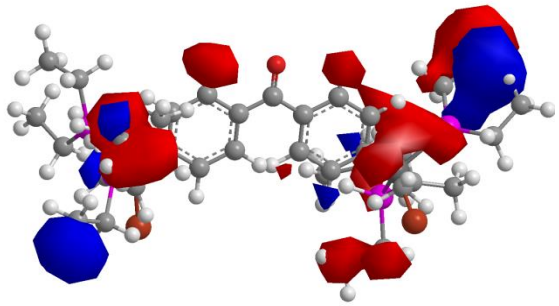

Figure 6: graphical representation of Huckel molecular orbitals of organoplatinum compound

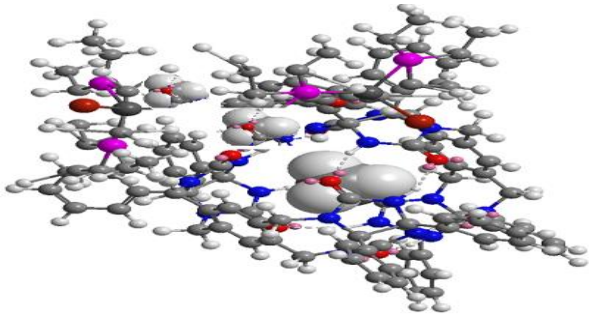

Figure 7: Organoplatinum supramolecular structure with encapsulated methane in its pore openings.

The most preferred binding sites of the organoplatinum (II) supramolecular metallacycle was determined by molecular simulation studies with experimental results. Figure 8a is a plot of the Pt(II) supramolecular metallacycle showing binding sites with reaction pathways. The major difference is between MTX1 and ASN 18 residues. The blue arrows show the reaction pathways while 8b shows the large binding site with volume/surface, an indication of its potency to effectively coordinate with other molecules to form supramolecular cages of polymeric geometry for drug delivery and energy application [15].

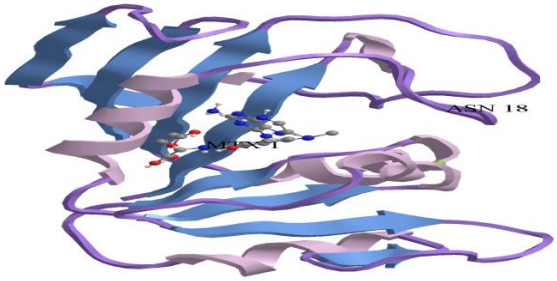

Figure 8: (a) Molecule showing binding sites with reaction path ways

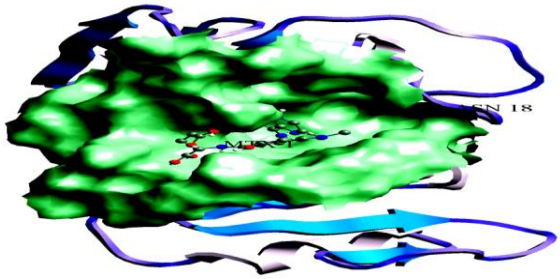

Figure 8: (b) Molecule showing binding site with surface

The different proton and carbon environment of the synthesized compound were analyzed by ^{1}H and ^{13}C [30] NMR analyses [17]. The ^{1}H NMR (100 Mhz; $CDCl_3$) spectrum of organoplatinum (II) compound in Figure 9a reveals a characteristic singlet at 0.00 ppm ascribed to the solvent peak. The formation of organoplatinum (II) compound is seen at 2.09 ppm of the phenyl protons. The observed peaks downfield of 7.55- 7.57 ppm corresponds to eight aromatic protons of the compound. In the ^{1}H NMR [31] spectrum of supramolecular metallacycle, the presence of multiplets in regions δ =1.63-1.66 and 1.0-1.04 pm (protons from $PtEt_3$ groups) suggest reaction of ligand 4,4'-dibromobenzophenone with two molecules of $Pt(PEt_3)_2$. In ^{13}C NMR spectrum (Figure 9b), the incorporation of $Pt(PEt_3)_2$ unit was observed in the appearance of a single signal at 30.77 ppm in ^{1}C NMR spectrum, indicating there was no isomer formed. There were satellite peaks in the spectrum because of spin-spin [23] coupling between ^{31}P and ^{195}Pt nuclei [11].

ISSN 0795 - 22066

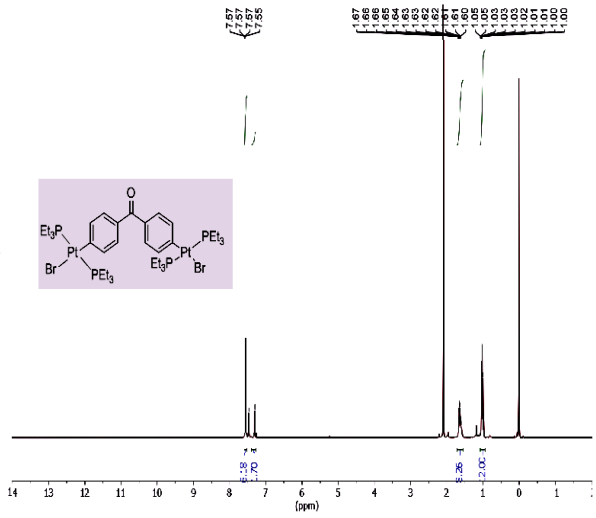

Figure 9a: ^{1}H NMR (100 Mhz; $CDCl_3$) spectrum

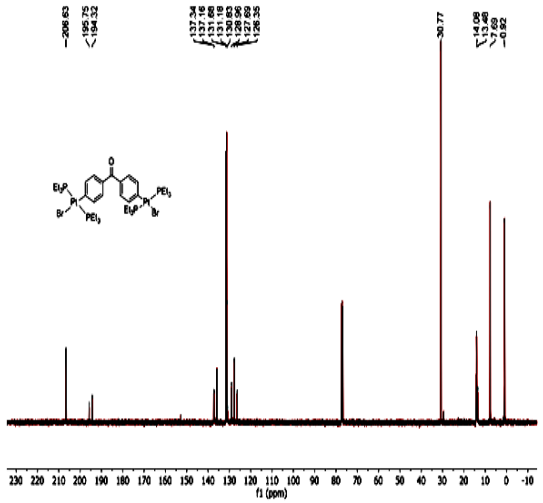

Figure 9b: ^{13}C NMR (100 Mhz; $CDCl_3$) spectrum

DISCUSSION

In coordination-driven [7] self- assembly convention, metal ion as acceptors and organic ligands as donors are combined by means of coordination bonds to form two-dimensional metallacycles and three-dimensional metallacages. Our group explored the self-assembly [32] process and combined three precursors to prepare the supramolecular platinum(II) metallacycle with square planar-core supported by two triethyl phosphine, one bromide and one benzophenone ligands. The optimized crystal structure from diverse models and coordination environments for this compound can be understood on the premise of the trend in ionic radii and related modification in coordination numbers of the cations. Modern drug discovery is capital intensive, lengthy, wasteful process with the low rate of novel therapeutic discovery, in spite of advances in technology and understanding of biological systems. The thought of utilizing calculations for molecular design goes back to the mid-1980s [33] in reports of Free Energy Perturbation calculation for the conversion of a molecule X to molecule Y for protein-ligand binding. The geometry optimized structure in Figures 4 and 5 give a stable two-dimensional arrangement of atoms within the organoplatinum molecule in its minimal energy state of 2.26 eV. The molecules are most reactive and stable with the lowest energy value. This was achieved utilizing diverse models such as DFT, molecular dynamics, degrees of freedom and organoplatinum binding sites affinities in the investigation. The NMR results in Figures 9a and 9b are an indication of the formation of a supramolecular organoplatinum metallacycle with 90% purity. Purity of this compound is required especially in the field of biomedical applications. This study showing the synthesized supramolecular organoplatinum metallacycle by coordination-driven self-assembly of non-covalent interactions with a 60 ° pyridyl ligand donor can further be developed to supramolecular metallacage in the mitigation of cancer cells.

CONCLUSION

We demonstrate the protocol of "coordination-driven self-assembly" for the construction of 120° supramolecular

ISSN 0795 - 22066

organoplatinum (II) metallacycle in solution under an inert atmosphere. The compound was characterized by ^{1}H and ^{13}C NMR spectroscopic techniques. The optimized structure of the supramolecular organoplatinum (II) metallacycle was ascertained by DFT method and molecular dynamics. The energy of formation was predicted based on features and atomic properties from optimized structures. The results from experiment and optimization protocols show that the coordination- driven self-assembled compound offers high reversible binding properties for designing smart surfaces that may find applications in catalysis, energy storage, sensing, and biomedicine.

REFERENCES

1. L. Chen, Q. Chen, M. Wu, F. Jiang and M. Hong (2015). Controllable coordination-driven self-assembly: From discrete metallacages to infinite cage-based frameworks. Acc. Chem. Res. 48(2): 201-210

2. K. Ghosh, J. Hu, H. S. White and P. J. Stang (2018). Coordination of multifunctional cuboctahedra via coordination-driven self-assembly. Journal of American Chemical Society 2009, 131, 6695-6697.

3. A. Bhat, E. Zangrando and P.S Mukherjee (2019). Coordination-driven self-assembly of discrete molecular nanotubular architectures. Inorg. Chem., 58(16), 11172-11179

4. E. G. Percastegui and V. Jancik (2020). Coordination-driven assemblies based on meso-substituted porphyrins: Metal-organic cages and a new type of meso-metallaporphyrin macrocycles. Coordination Chemistry Reviews 407, 213165,1-31

5. M. Mon, R. Bruno, S. Sanz-Navarro, C. Negro, J. Ferrando-Soria, L. Bartella, L. D. Donna, M. Prejano, T. Marino, A. Leyva-Perez, D. Armentano and E. Pardo (2020). Hydrolase-like catalysis and structural resolution of natural products by a metal-organic framework. Nature Communications. 11(3080), 1-9

6. L. Ma, J. Q. Han, W. Jia and Y. Han (2018). Coordination-driven self-assembly vs dynamic covalent chemistry: versatile methods for the synthesis of molecular metallarectangles, Beilstein J.Org. Chem., 14, 2027-2034

7. Y. Huang, D. Wu, M. Bao, B. Li and H. Liang (2019). Coordination driven self-assembly for enhancing the biological stability of nobiletin. Journal of Molecular Liquids 294: 111420 1-8

8. H. Zhao, Y. Zhao, J. Xu, X. Feng, G. Liu, Y. Zhao and X. Yang (2020). Programmable co-assembly of various drugs with temperature sensitive nanogels for optimizing combination chemotherapy. Chemical Engineering Journal 398 125614: 1-13.

9. Y. Sun, F. Ding, Z. Chen, R. Zhang, C. Li, Y. Xub, Y. Zhang, R. Ni, X. Li, G. Yang, Y. Sun and P. J. Stang (2019). Melanin-dot-mediated delivery of metallacycle for NIR-II/photoacoustic dual-model imaging-guided chemo-photothermal synergistic therapy, PNAS, 116(34),16729-16735

10. J. Zhao, Y. Cao and L. Zhang (2020). Exploring the computational methods of protein-ligand binding site prediction. Computational and Structural Biotechnology Journal 18: 417-426

11. N. Singh, J. Singh, D. Kim, D. H. Kim, E. Kim, M. S. Lah and K. Chi (2018). Coordination-driven self-assembly of heterotrimetallic barrel and bimetallic cages using a cobalt sandwich-based tetratopic donor. Inorg. Chem., 2018, 57(7), 3521-3528.

ISSN 0795 - 22066

12. C. R. P. Fulong, S. Kim, A. E. Friedman and T. R. Cook (2019). Coordination-driven self-assembly of silver (I) and gold(I) rings: synthesis, characterization, and photophysical studies. Frontiers in Chemistry, 7, 567,

13. E. Semitut, V. Komarov, T. Sukhikh, E. Filatov and A. Potapov (2016). Synthesis, crystal structure and thermal stability of 1D linear silver(I) coordination polymers with 1,1,2,2-tetra(pyrazol-1-yl)ethane. Crystals 6(11): 138-150

14. M. Ebara and K. Uto (2016). 8-Gold nanomaterials for gene therapy. Polymers and Nanomaterials for gene therapy.189-214

15. X. Yang, Y. Wang, R. Byrne, G. Schneider and S. Ynag (2019). Concept of artificial intelligence for computer-assisted drug discovery. Chemical Reviews 119, 10520-10594 DOI: 10.1021/acs.chemrev.8b00728.

16. A. Jasz, A. Rak, I. Ladjanszki and G. Cserey (2019). Optimized GPU implementation of merck molecular force field and universal force field. Journal of Molecular Structure 1188: 227-233

17. K. Singh, A. Gangrade, A. Jana, B. B. Mandal and N. Das (2019). Design, synthesis, characterization, and antiproliferative activity of organoplatinum compounds bearing a 1,2,3-triazole ring. ACS Omega 4: 835-841

18. X. Ai, E. Evans, S. Dong, A. J. Gillett, H. Guo, C. Yingxin, T.J.H. Hele, R. H. Friend and F. Li (2018). Efficient radical-based light-emitting diodes with doublet emission. Nature 563(7732), 536-540

19. W. Zheng, L. J. Chen, G. Yang, Sun B., Wang X., Jiang B., Yin GQ, Zhang L., Li X., Liu M., Chen G., and Yang H.B. (2016). Construction of smart supramolecular polymeric hydrogels crosslink by discrete organplatinum (II) metallacycles via post assembly polymerization. J. Am. Chem. Soc. 138: 4927-4937

20. E.E. Ebenso, A. Taner, K. Fatima, C. Necmettin and L. Ian (2010). Quantum chemical studies of some rhodanine azosulpha drugs as corrosion inhibitors for mild steel in acidic medium. International Journal of Quantum Chemistry. 110(5) 1003-1018 DOI: 10.1002/qua.22249

21. M. Karthikeyan, B. Ramakrishna, S. Velaiyadevan, D. Divya and B. Manimaran (2018).Amide-functionalized chalcogen-bridged flexible tetranuclear rhenacycles: synthesis, characterization, solvent effect on the structure, and guest binding . ACS Omega 3, 3257-3266

22. A. Pothig and A. Casini (2019). Recent developments of supramolecular metal-based structures for applications in cancer therapy and imaging. Therenostics 9(11): 3150-3169 DOI: 10.7150/thno.31828.

23. M. Zhang, S. Yina, J. Zhang, Z. Zhoua, M. L, Saha, C. Lu and P. J. Stang (2017). Metallacycle-cored supramolecular assemblies with tunable fluorescence including white-light emission. PNAS 114(12): 3044-3049

24. B. Breiner, J. Clegg and J. R. Nitschke (2011). Reactivity Modulation in Container Molecules. Chemical Science 2(1): 51-56

25. Y. Lin, M. Chuang, P. Wu, C. Chen, S. Jeyachandran, S. Lo, H. Huang and M. Hou (2016). Selective recognition and stabilization of new ligands targeting the potassium form of the human telomeric G-quadruplex DNA. Scientific Reports 6:31019 , 1-14 DOI: 10.1038/srep31019

26. V. Kumar (2008). Chapter three- Metal encapsulated clusters of silicon: silicon fullerenes and other polyhedral forms. Nano silicon, 114-148

ISSN 0795 - 22066

27. L. Pirondini, F. Bertolini, B. Cantadori, F. Ugozzoli, C. Massera and E. Décanale (2002). Design and self-assembly of wide and robust coordination cages. PNAS 99(8): 4911-4914

28. A. Kumari, R. Singla, A. Guliani and S.K. Yadav (2014). Nano encapsulation for drug delivery. EXCLI J. 13: 265-286 PMC4464443.

29. H. Wang, H. Yeh, Y. Chen, Y. Lai, C. Lin, K. Lu, R. Ho, B. Li, C. Lin and D. Tsai (2018) Thermal stability of metal-organic frameworks and encapsulation of CuO nanocrystals for highly active catalysis. ACS Appl. Mater. Interfaces 10: 9332-9341

30. N. B. Debata, D. Tripathy and H. S. Sahoo (2019). Development of coordination driven self-assembly discrete spherical ensembles. Coordination Chemistry Reviews 387: 273-298

31. G. R. Fulmer, A. J. M. Miller, N. H. Sherden, H. E. Gottlieb, A. Nudelman, B. M. Stoltz, J. E. Bercaw and K. I. Goidberg (2010). NMR chemical shifts of trace impurities: common laboratory solvents, organics, and gases in deuterated solvents relevant to the organometallic chemist. Organometallics 29(9): 2176-2179

32. X. Du, J. Zhou, J. Shi and B. Xu (2015). Supramolecular hydrogelators and hydrogels: from soft matter to molecular biomaterials. Chem. Rev.115 (24): 13165-13307 DOI: 10.1021/acs.chemrev.5b00299

33. Z. Cournia, B. Alen and W. Sherman (2017). Relatively binding free energy calculations in drug delivery: recent advances and practical consideration. J. Chem. Inf. Model 57(12): 2911-2937.

ISSN 0795 - 22066